APEX (Aqueous Photochemistry of Environmentally-occurring Xenobiotics): A Free Software Tool to Predict the Kinetics of Photochemical Processes in Surface Waters.

M. Bodrato, D. Vione.
APEX (Aqueous Photochemistry of Environmentally-occurring Xenobiotics): A Free Software Tool to Predict the Kinetics of Photochemical Processes in Surface Waters.
ENVIRONMENTAL SCIENCE. PROCESSES & IMPACTS (PRINT) (2014) 16
DOI: 10.1039/c3em00541k

APEX (Aqueous Photochemistry of Environmentally-occurring Xenobiotics): A free software tool to predict the kinetics of photochemical processes in surface waters

Marco Bodrato[a] and Davide Vione*[b,c]

The APEX software predicts the photochemical transformation kinetics of xenobiotics in surface waters as a function of: photoreactivity parameters (direct photolysis quantum yield and second-order reaction rate constants with transient species, namely $^{\bullet}OH$, $CO_3^{-\bullet}$, $^1O_2$ and the triplet states of chromophoric dissolved organic matter, $^3CDOM^*$); water chemistry (nitrate, nitrite, bicarbonate, carbonate and dissolved organic carbon, DOC), and water depth (more specifically, the optical path length of sunlight in water). It applies to well-mixed surface water layers, including the epilimnion of stratified lakes, and the output data are average values over the considered water column. Based on intermediate formation yields from the parent compound *via* the different photochemical pathways, the software can also predict intermediate formation kinetics and overall yield. APEX is based on a photochemical model that has been validated against available field data of pollutant phototransformation, with good agreement between model predictions and field results. The APEX software makes allowance for different levels of knowledge of a photochemical system. For instance, the absorption spectrum of surface water can be used if known, or otherwise it can be modelled from the values of DOC. Also the direct photolysis quantum yield can be entered as a detailed wavelength trend, as a single value (constant or average), or it can be defined as a variable if unknown. APEX is based on the free software *Octave*, and it is freely available as Electronic Supplementary Information of this article. Additional applications are provided within APEX to assess the σ-level uncertainty of the results and the seasonal trend of photochemical processes.

1 Introduction

Photochemical reactions are important pathways for the removal of biorefractory compounds from surface waters, including xenobiotics such as pesticides, pharmaceuticals and personal care products. Photoinduced reactions are usually divided into direct and indirect (or sensitised) photolysis processes.[1,2]

In the case of direct photolysis, absorption of sunlight by a compound triggers its phototransformation because of phenomena such as bond breaking and photoionisation.[3] Indirect or sensitised photolysis does not require radiation absorption by the compound. Sunlight is rather absorbed by photoactive components called photosensitisers (such as nitrate, nitrite and chromophoric dissolved organic matter, CDOM), which produce reactive transient species including $^{\bullet}OH$, $CO_3^{-\bullet}$, $^1O_2$ and CDOM triplet states, $^3CDOM^*$.[4-7] Specifically, the formation of $CO_3^{-\bullet}$ requires oxidation of carbonate and bicarbonate by $^{\bullet}OH$ and of carbonate by $^3CDOM^*$.[8] Surface-water photosensitisers also include Fe species,[9-11] of which the chemistry and photochemistry at neutral pH is still poorly known. However, considering the likely interaction between Fe and CDOM in photo-Fenton processes,[12] a fraction of Fe photochemistry at circumneutral pH would be taken into account with CDOM photoreactions.[5]

Direct and sensitised photolysis induce transformation of water-dissolved pollutants, yielding different intermediates depending on the actual pathway involved.[13-15] Even when there is a large overlap between intermediates produced by different processes, the associated formation yields may be strongly process-dependent.[16-18]

We have recently developed a photochemical model that predicts photochemical reactions and pollutant phototransformation as a function of water chemistry and of the optical path length of sunlight in water, the latter being proportional to water depth. The model relies as key input data on pollutant photoreactivity parameters such as the direct photolysis quantum yield and the second-order reaction rate constants with $^{\bullet}OH$, $CO_3^{-\bullet}$, $^1O_2$ and $^3CDOM^*$.[19,20] More recently the model was implemented into the APEX software, which is described in this paper and can be freely downloaded. Although free packages are available to compute the kinetics of direct photolysis,[21,22] to our knowledge APEX is the only software linking water chemistry and depth with both direct and indirect photochemistry.

2 The photochemical model for surface waters

The photochemical model in use with APEX considers direct photolysis and indirect photochemistry by reaction with $^{\bullet}OH$, $CO_3^{-\bullet}$, $^1O_2$ and $^3CDOM^*$. Here only a brief account of the model is reported. Details of the model equations for the different photochemical processes are provided in the User's Guide of APEX, which is included together with the whole software package as Electronic Supplementary Information (ESI) of this paper.

The model considers the generation of $^{\bullet}OH$ by irradiation of nitrate, nitrite and CDOM, the formation of $^3CDOM^*$ and $^1O_2$

upon CDOM irradiation, and the production of $CO_3^{-\bullet}$.[23,24] The latter takes place upon oxidation of carbonate and bicarbonate by $^{\bullet}OH$ and of carbonate by ^{3}CDOM*.[8] The main reactions are reported below (ISC = inter-system crossing):

$$NO_3^- + h\nu + H^+ \rightarrow {}^{\bullet}OH + {}^{\bullet}NO_2 \quad (1)$$

$$NO_2^- + h\nu + H^+ \rightarrow {}^{\bullet}OH + {}^{\bullet}NO \quad (2)$$

$$CDOM + h\nu \rightarrow {}^1CDOM^* \xrightarrow{ISC} {}^3CDOM^* \quad (3)$$

$$^3CDOM^* + O_2 \rightarrow CDOM + {}^1O_2 \quad (4)$$

$$^{\bullet}OH + HCO_3^- \rightarrow H_2O + CO_3^{-\bullet} \quad (5)$$

$$^{\bullet}OH + CO_3^{2-} \rightarrow OH^- + CO_3^{-\bullet} \quad (6)$$

$$^3CDOM^* + CO_3^{2-} \rightarrow CDOM^{-\bullet} + CO_3^{-\bullet} \quad (7)$$

The quantum yield of $^{\bullet}OH$ generation by nitrate depends on pH but it does not vary in the solar UV range.[25] In contrast, the $^{\bullet}OH$ quantum yield by nitrite decreases with increasing wavelength, from 0.068 at 300 nm to 0.025 at 350 nm.[26]

The pathways leading to the production of $^{\bullet}OH$ from CDOM are not yet completely clear. A fraction of $^{\bullet}OH$ production by CDOM is expected to involve H_2O_2,[27] photogenerated upon *e.g.* dismutation of $O_2^{-\bullet}$.[28] Direct photolysis of H_2O_2 [29] or Fenton and photo-Fenton processes [9,12] could then be involved in $^{\bullet}OH$ generation. As far as H_2O_2-independent $^{\bullet}OH$ production by CDOM is concerned, oxidation of water or OH^- by ^{3}CDOM* is possible [30] but its actual occurrence in CDOM photochemistry is still to be proven. Anyway, the model takes into account experimental data of $^{\bullet}OH$ photogeneration by surface-water CDOM,[5] whatever the actual generation pathway. By this approach one would partially take the Fe chemistry into account, because the photo-Fenton reactions would involve complexes between Fe(III) and organic ligands.[9,12] A comprehensive description of Fe photochemistry will require a better understanding of the speciation of this element in surface waters.

In addition to the formation of reactive species, scavenging reactions are also taken into account. The model considers the scavenging of $^{\bullet}OH$ by DOM, bicarbonate, carbonate, bromide and nitrite (the latter being a very minor pathway),[31,32] the reaction between $CO_3^{-\bullet}$ and DOM,[8] and the thermal deactivation of $^1O_2$ upon collision with the solvent.[33] In the case of ^{3}CDOM*, it is used a pseudo-first order decay constant determined for aerated aqueous systems,[34] which is higher than for anoxic waters due to reaction (4). This choice is due to the fact that the model applies to the surface water layer that is usually well oxygenated. An overall scheme of the main modelled reactions is provided below (note that "td" means thermal deactivation).

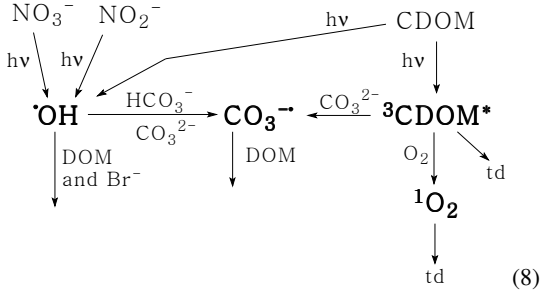

(8)

A major issue in the modelling of photochemical processes in surface waters is the competition for sunlight irradiance between different light-absorbing species, and most notably between nitrate, nitrite and CDOM. The latter is the main sunlight absorber in the 300-500 nm interval,[35] which is most significant from the point of view of surface-water photochemistry.[36] Competition for irradiance is taken into account in the model within a Lambert-Beer approach. Absorbance values are easier to be calculated than the absorbed spectral photon flux densities, but the latter are the basis for the assessment of photochemical reaction rates.[37] A relatively simple exponential relationship exists between absorbance and absorbed spectral photon flux density, for any wavelength λ, only when the overall values referred to the whole solution are taken into account ($A_{tot}(\lambda)$ and $p_a^{tot}(\lambda)$, respectively). The relationship reads as follows:[37]

$$p_a^{tot}(\lambda) = p°(\lambda) \cdot [1 - 10^{-A_{tot}(\lambda)}] \quad (9)$$

where $p°(\lambda)$ refers to the incident spectral photon flux density of sunlight. For any solute *i*, the ratio of its absorbed spectral photon flux density $p_a^i(\lambda)$ to $p_a^{tot}(\lambda)$ is equal to the ratio of its absorbance $A_i(\lambda)$ to the total absorbance $A_{tot}(\lambda)$. Therefore, $p_a^i(\lambda)$ can be expressed as follows:[38]

$$p_a^i(\lambda) = \frac{A_i(\lambda)}{A_{tot}(\lambda)} p°(\lambda) \cdot [1 - 10^{-A_{tot}(\lambda)}] \quad (10)$$

Integration of $p_a^i(\lambda)$ over wavelength gives the photon flux absorbed by *i*, P_a^i. If the solute *i* is photochemically active (*e.g.* nitrate, nitrite or CDOM), the calculation of the formation rate of the reactive species *j* upon irradiation of *i* requires the knowledge of the quantum yield $\Phi_{j,i}(\lambda)$.[37] In some cases, such as for nitrite,[26] the wavelength trend of the quantum yield is known and the formation rate of *j* by *i* can be calculated as follows:

$$r_{j,i} = \int_{\lambda} \Phi_{j,i}(\lambda) \frac{A_i(\lambda)}{A_{tot}(\lambda)} p°(\lambda) \cdot [1 - 10^{-A_{tot}(\lambda)}] \, d\lambda \quad (11)$$

If the quantum yield does not vary with wavelength or if the wavelength trend of $\Phi_{j,i}(\lambda)$ is not known, a single numerical value can be used that is placed outside the integral. In this case, one obtains the simpler equation $r_{j,i} = \Phi_{j,i} P_a^i$.

This approach can be used for the photoactive compounds (nitrate, nitrite, CDOM) and the photogenerated reactive species ($^{\bullet}OH$, $^1O_2$ and ^{3}CDOM*, the case of $CO_3^{-\bullet}$ being a bit different as it is not directly generated upon irradiation, see scheme 8). From the formation-transformation budget one can obtain the steady-state concentration [*j*] of each reactive species in the irradiated volume. The latter consists of a more intensely illuminated fraction near the surface and of a darker one at depth, thus the concentration of *j* is expected to decrease when passing from the illuminated surface layer to darker environments.[32,39] The calculated steady-state concentration [*j*] is an average over the whole volume, with contributions from both the upper and the bottom layers. The model applies to well-mixed surface waters such as rivers or the epilimnion of stratified lakes, where the chemical composition shows limited variations with depth.[40,41]

To make an instance, in the case of $^{\bullet}OH$ the relevant steady-state concentration can be expressed as follows:[19]

$$[^{\bullet}OH] = \frac{r_{^{\bullet}OH}^{NO_3^-} + r_{^{\bullet}OH}^{NO_2^-} + r_{^{\bullet}OH}^{CDOM}}{\sum_i k_{Si}\,[S_i]} \qquad (12)$$

where the contribution of the photosensitisers to $^{\bullet}$OH generation is considered, and $\sum_i k_{Si}\,[S_i]$ is the first-order rate constant of $^{\bullet}$OH scavenging by DOM, HCO_3^-, CO_3^{2-}, Br^- and NO_2^-.

The degradation kinetics of a given xenobiotic P by the reactive species *j* can be expressed by the pseudo-first order rate constant $k'_{P,j} = k_{P,j}\,[j]$, where $k_{P,j}$ is the second-order rate constant of the reaction between P and *j*. The $k_{P,j}$ values between P and $^{\bullet}$OH, $^1O_2$, $CO_3^{-\bullet}$ and ^{3}CDOM* should be known because they are key input data for the software (*vide infra*).

For the direct photolysis, the transformation rate of P can be obtained with a slightly modified version of equation (11):[42]

$$r_P = \int_{\lambda} \Phi_P(\lambda)\,\frac{A_P(\lambda)}{A_{tot}(\lambda)}\,p^{\circ}(\lambda)\cdot[1-10^{-A_{tot}(\lambda)}]\;d\lambda \qquad (13)$$

where $\Phi_P(\lambda)$ is the quantum yield of P direct photolysis. Similar observations as above apply if the wavelength trend of the quantum yield is known, or if a constant or average value is used instead. The pseudo-first order rate constant of the direct photolysis is $k'_{P,phot} = r_P\,[P]^{-1}$, which is independent of [P] if the latter is sufficiently low.[11]

The overall rate constant of P transformation *via* the different photochemical processes is $k'_P = \sum_j k'_{P,j}$, where the sum on *j* includes the direct photolysis.

The model can also be applied to the formation of intermediates.[18] In particular, assume that the by-product B can be formed from P in the photochemical process *j* (direct photolysis or reaction with $^{\bullet}$OH, $CO_3^{-\bullet}$, $^1O_2$ or ^{3}CDOM*), with yield $\eta_{P\Rightarrow B,j}$ (which is another input datum of the software). The corresponding rate constant of B formation is $k'_{B,j} = (\eta_{P\Rightarrow B,j})\,k'_{P,j}$. It is thus possible to calculate the overall rate constant of photochemical B formation and its overall formation yield from P (equations 14 and 15, respectively):[18]

$$k'_B = \sum_j [(\eta_{P\Rightarrow B,j})\,k'_{P,j}] \qquad (14)$$

$$\eta_{P\Rightarrow B} = \frac{\sum_j [(\eta_{P\Rightarrow B,j})\,k'_{P,j}]}{\sum_j k'_{P,j}} = \frac{k'_B}{k'_P} \qquad (15)$$

The theoretical framework provided so far could well be applied to steady irradiation conditions. However, this is not the case for the outdoor environment where, apart from unpredictable meteorology issues, there are at least diurnal and seasonal cycles to be taken into account. Therefore, it is important to mention that the model uses a standardised time unit, intended on the one side to provide a reference time of definite duration and, on the other side, to give insight into the day-night cycle. That unit is a summer sunny day (SSD), which corresponds to mid-latitude (45°) 15 July under fair-weather conditions.[42] The model output in SSD units allows a rather straightforward comparison with field data obtained during summertime under mid-latitude conditions. Further calculations are needed to get insight into *e.g.* the expected seasonal trend. A tool to approximately calculate mid-latitude photochemical kinetics in different months of the year is provided with the APEX package (see ESI and *vide infra*).

The model has been applied to the photochemical fate of a variety of xenobiotic compounds in surface waters. It was validated by comparison between its predictions and field data of photochemical transformation, when available. The following table reports the comparisons that have been carried out so far, with a good agreement between predictions and field data.

Table 1. Comparison between model predictions and field data, for different compounds and different locations.

Substrate	$t_{½}$, model (days)	$t_{½}$, field (days)	Location	Reference
2,4-Dichloro-6-nitrophenolate	6.3±2.3	8.4±0.5	Rhône delta (S. France)	43
Ibuprofen	58±9	60-110	Greifensee (Switzerland)	44,45
4-Chloro-2-nitrophenolate	5.5±1.5	6.4±0.3	Rhône delta (S. France)	46,47
Carbamazepine	115±40	140±50	Greifensee (Switzerland)	45,48
MCPA	12±1	10±2	Rhône delta (S. France)	49
Atrazine	17±4 64±18	20-21 67-100	Chesapeake Bay, MD, USA (2 sites)	50,51

3 The APEX software

APEX is based on the *Octave* software, which is available for free download (*http://www.gnu.org/software/octave*, and *http://sourceforge.net/projects/octave/files/Octave%20Windows%20binaries/* for Windows versions). Therefore, *Octave* should be installed before running APEX.

An overall scheme of the APEX architecture is depicted in Figure 1. The different parts will be described in the next sections, but a more complete and operationally-oriented description is provided in the User's Guide (see ESI). Note that the software can draw a 3D plot or produce a table with the same output values. The two tasks are carried out by two different functions, namely *plotgraph* and *savetable*.

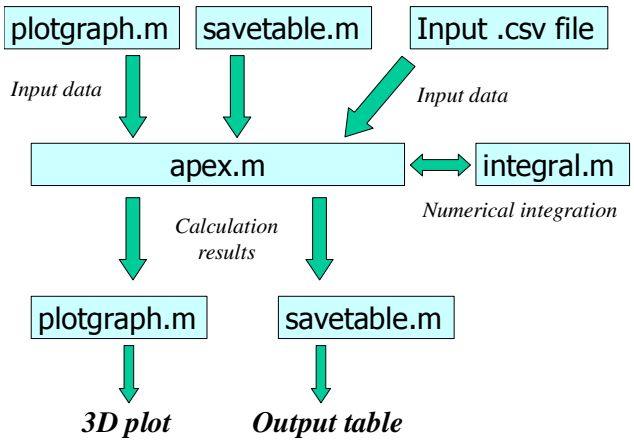

Figure 1. General structure of the APEX software.

3.1 Input file

Key input data are those describing the photochemical reactivity of the xenobiotic compound of interest: absorption spectrum, photolysis quantum yield and second-order reaction rate constants with $^{\bullet}OH$, $CO_3^{-\bullet}$, $^1O_2$ and $^3CDOM^*$. In some cases the needed data are available from the literature.[8,52,53] To fill up possible gaps, an experimental protocol has been developed for the experimental determination of all needed parameters. Such a protocol has been applied for instance to all the compounds listed in Table 1 and it is described in the relevant references. The protocol can be adapted to compounds undergoing acid-base equilibria. For instance, in the case of the sunlight filter benzophenone-4 (pK_a ~ 7) the kinetic parameters of interest have been determined separately for the acidic and the basic species, which allowed photochemical modelling as a function of pH.[54]

Some input data are functions of the wavelength, such as the absorption spectrum (molar absorption coefficients) of the target compound. These data are included in tabular form in an input .csv file, of which some examples for different xenobiotics are provided in ESI with file names of the kind *compoundname.csv*. These files also contain the molar absorption coefficients of nitrate and nitrite, the wavelength trend of the quantum yield of $^{\bullet}OH$ generation by nitrite, and a standard spectral photon flux density of sunlight. The latter corresponds to a mid-latitude irradiance of 22 W m^{-2} in the 290-400 nm wavelength interval.[55]

In the .csv input file it is also possible to include, if available, the photolysis quantum yield of the target compound (with the possibility to report wavelength-dependent values if applicable or known) and the absorption spectrum of water, expressed as the absorbance over an optical path length of 1 cm. Considering that photochemical reactions are faster near the water surface,[32] the absorption spectrum of a water sample taken from the surface layer should be inserted here, if available. If such a spectrum is not available, the software will model it on the basis of the content of dissolved organic carbon (DOC, also termed as NPOC, non-purgeable organic carbon). Indeed, the absorption spectra of surface waters are exponentially decaying functions with a reasonably good correlation between absorbance and DOC.[56] To tell the software that the absorption spectrum is to be modelled instead of taken from the input file, one should insert "-1" overall in the file column related to the water absorbance.

As far as the direct photolysis quantum yield of the xenobiotic compound is concerned, there is the possibility to insert wavelength-dependent values, a constant value throughout, or to define the quantum yield as a variable if its value is not known. Definition of the quantum yield as variable should be made within the *plotgraph* and *savetable* functions. To enable this, one should insert "-1" in the whole quantum yield column of the input .csv file, otherwise the software will read with priority the data contained in that column.

The input file should be placed in the same folder that contains all the APEX files.

3.2 The *plotgraph* function

This function is provided as a file (*plotgraph.m*) that can be opened and modified with standard text/notepad applications. Use of word processors is not recommended because they could add text strings when saving the files. Such strings would not be recognised and could cause errors when running APEX.

The *plotgraph* function draws a 3D plot, and the X and Y variables have to be chosen among parameters of water chemistry and photochemical reactivity of the target compound. The relevant water parameters are the path length of sunlight (depth dependent, *vide infra*), the molar concentration values of nitrate, nitrite, carbonate and bicarbonate, and the DOC or NPOC (units of mg C L^{-1}). The reactivity parameters are the photolysis quantum yield (if not already specified in the input .csv file), the second-order reaction rate constants between the target compound and $^{\bullet}OH$, $CO_3^{-\bullet}$, $^1O_2$ and $^3CDOM^*$, and (if available) the formation yields of an intermediate *via* the relevant photochemical pathways. Note that the reactivity data of the parent compound are needed to calculate intermediate formation kinetics, while the yields of the intermediate are not required to compute the transformation kinetics of the parent compound.

For each of the parameters related to water chemistry, compound photoreactivity or intermediate formation, one should either insert a known numerical value (or 0 if that value is negligible or not available), or define the relevant quantity as X or Y variable. For X and Y one should also define the range of variation, namely minimum and maximum values as well as step size. The format is *minimum:step:maximum*. The step size defines the grid density of the plot. A smaller step (higher density) enables better resolution and nicer aesthetic effect, but it also requires longer computational time. Indeed, if the step size of both X and Y is decreased by a factor of 10, the number of calculations (and time as a consequence) is multiplied by 100.

The Z variable to be plotted as a function of X and Y can be chosen within a list of 36 possible options, referred to either a single photochemical pathway (*e.g.* $^{\bullet}OH$ or $^1O_2$) or to the overall photochemical behaviour of the substrate or intermediate. Possible choices are: substrate half-life times and pseudo-first order transformation rate constants; steady-state concentrations of $^{\bullet}OH$, $CO_3^{-\bullet}$, $^1O_2$ and $^3CDOM^*$; pseudo-first order formation rate constants of the intermediate and its overall formation yield, as

well as the fractions of substrate transformation and intermediate formation that are accounted for by each single photochemical pathway. The list of choices is closed, but it is relatively wide to enable the use of the graphical option in many cases of interest.

Within the *plotgraph* function one should also specify the name of the input .csv file. At this point, in most cases the procedure is over and one can save the *plotgraph.m* file and exit it. However, the file also contains values of the quantum yields of $^{\bullet}OH$, $CO_3^{-\bullet}$, $^1O_2$ and ^{3}CDOM* generation by irradiated CDOM. They have been derived from studies dealing with irradiation of natural water samples,[5,8,57] but the relevant values could change in different environments. Therefore, if one needs to use CDOM-related quantum yields that have been measured in a particular environment, the existing data can be modified.

3.3 The *savetable* function

This function is intended to produce a table instead of a plot, out of the same calculations. Many issues already cited in the case of *plotgraph* hold here as well: choice of the X and Y variables and definition of their range and step size; introduction of numerical values for the additional parameters related to water chemistry and substrate photoreactivity/intermediate formation; definition of the name of the input .csv file. The *savetable.m* file can be opened, modified and saved with the same applications used for *plotgraph.m*.

The main difference is that here one has not to choose the Z variable, because all the possible output quantities (half-life times, pseudo-first order rate constants, steady-state concentrations and so on) will appear in the output table. An advantage that can be connected with the use of *savetable* compared to *plotgraph* is the availability of actual numerical values in the output table. These values allow further calculations to be carried out, including model errors and seasonal trends (*vide infra*). The higher flexibility enabled by the tables also allows the extension of calculations to reactive species that were not included in the original model. An example is represented by the transients $^{\bullet}NO_2$, $Br_2^{-\bullet}$ and $Cl_2^{-\bullet}$, which can be produced by interaction of some of the modelled reactive species (*e.g.* $^{\bullet}OH$ and/or ^{3}CDOM*) with nitrite, bromide and chloride.[54,58,59] On this basis, and upon addition of further equations derived from dedicated experiments and kinetic modelling, it was possible to use the output tables as starting points to model the environmental occurrence of the additional transients. The *savetable* function has also been used to model separately the photochemical reaction kinetics of the acidic and basic forms of benzophenone-4, by which the expected impact of pH on photochemistry could be computed by additional calculations.[54]

A further similarity with *plotgraph* is that the formation quantum yields of $^{\bullet}OH$, $CO_3^{-\bullet}$, $^1O_2$ and ^{3}CDOM* by CDOM are also reported in *savetable*. If needed, the existing values can be modified with new ones, derived for instance by irradiation of water samples from a definite environment. This will improve the accuracy of model predictions for photochemical processes taking place in that environment.

3.4 Numerical calculations

The *apex.m* function makes calculations on the basis of input data and instructions, using the model equations that are listed in detail in the User's Guide (see ESI). Many of the relevant equations require integration over wavelength, which is carried out numerically by the *integral.m* function. Generally speaking, the user does not need to modify the *apex.m* file. However, a reason to do so could be the need to modify scavenging/deactivation rate constants of the transients, if measured data from a particular environment are available.

3.5 Running APEX under *Octave*

As specified before, APEX is not a stand-alone application but it requires the free software *Octave* to be used. *Octave* has a DOS-like interface, thus it is highly advisable to place the APEX package in a folder that is easily reached by use of DOS commands (*e.g.*, C:\Apex). The figure below shows two examples on how to run *plotgraph* and *savetable*, after all the relevant issues related to input data and instructions have been carried out as described in sections 3.1-3.3.

```
octave-3.2.4.exe:1> cd c:\Apex
octave-3.2.4.exe:2> plotgraph()
```
(a)

```
octave-3.2.4.exe:1> cd c:\Apex
octave-3.2.4.exe:2> savetable("output.csv")
```
(b)

Figure 2. Commands for running the *plotgraph* **(a)** and *savetable* **(b)** functions within Octave.

In both cases, the first instruction calls the folder that contains the files *plotgraph.m* and *savetable.m*. Note that if no file name is specified within *plotgraph* (command: plotgraph() as shown in Figure 2a), the output is shown in a window on the screen that allows for instance free rotation of the plot to get the best perspective. It is also possible to specify a file name in which to save the plot (recommended format is .pdf, *e.g.* plotgraph("output.pdf")), but in this case no further rotation is allowed. In the case of *savetable*, a file name for the output table has to be specified. Recommended output format is .csv.

Figure 3 reports two 3D plots generated by *plotgraph*. Compared to the raw output, axis titles were added by means of a standard drawing application. If one wishes a different format or appearance of the plots, it is suggested to run *savetable* and then to use the output table within dedicated software for plot drawing.

Atrazine, the degradation kinetics of which is modelled in Figure 3, is transformed in surface waters mainly by direct photolysis (quantum yield of $(1.6\pm0.2)\cdot10^{-2}$) and reactions with $^{\bullet}OH$ (second-order rate constant of $(2.7\pm0.3)\cdot10^9$ M^{-1} s^{-1}) and ^{3}CDOM* ($(1.4\pm0.1)\cdot10^9$ M^{-1} s^{-1}). The intermediate DEAOH (4-amino-2-hydroxy-6-isopropylamino-1,3,5-triazine) is formed from ATZ by direct photolysis (yield 0.10±0.01) and reaction with $^{\bullet}OH$ ($(8.6\pm4.6)\cdot10^{-2}$). The DEAOH yields of other processes are negligible.[51] The rate constant of ATZ has a minimum as a function of DOC (Figure 3a), because of the prevalence of direct photolysis and $^{\bullet}OH$ reaction at low DOC and of ^{3}CDOM* at high DOC. The fact that ^{3}CDOM* is not involved in DEAOH

formation explains why, differently from ATZ, the DEAOH rate constant steadily decreases with increasing DOC (Figure 3b). Organic matter inhibits both direct photolysis and reaction with $^{\bullet}OH$, the former because of competition for irradiance between ATZ and CDOM and the latter because of $^{\bullet}OH$ scavenging by DOM. Furthermore, high DOC also implies high CDOM that understandably enhances the ^{3}CDOM*-mediated processes.

The involvement of different photochemical pathways in the degradation of organic pollutants is highly substrate-dependent. For instance, aniline mainly undergoes degradation by reaction with $CO_3^{-\bullet}$ and its photoinduced transformation would be favoured in low-DOC waters rich in carbonate and bicarbonate.[19,20]

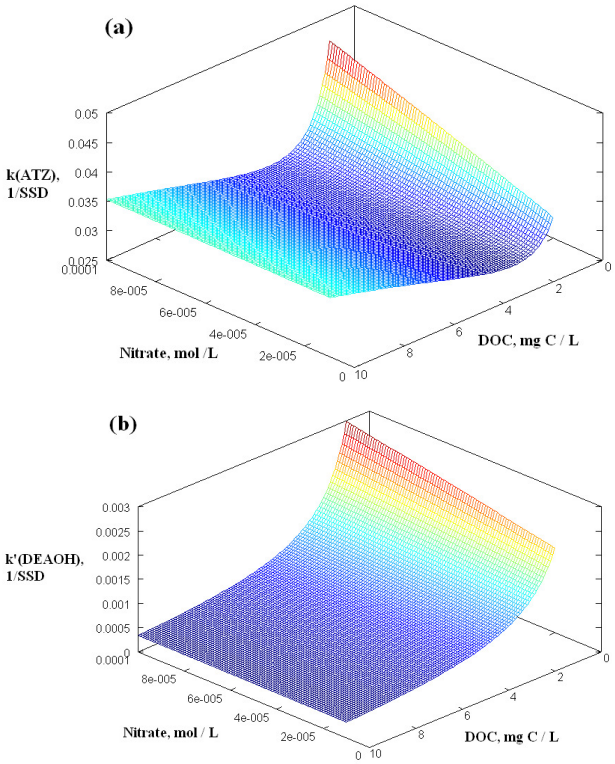

Figure 3. **(a)** Pseudo-first order degradation rate constant of atrazine (ATZ) as a function of nitrate concentration and of DOC. Other conditions: 2 m path length, 1 µM nitrite, 1 mM bicarbonate, 10 µM carbonate.
(b) Pseudo-first order formation rate constant of 4-amino-2-hydroxy-6-isopropylamino-1,3,5-triazine (DEAOH) as a function of nitrate and DOC. Other conditions are as above.

3.6 Determination of model uncertainty

Among the input data, those concerning the photochemical reactivity of the target compound are derived from experiments and they are affected by error. Further uncertainty is related to the experimentally-derived values of quantum yields of photochemical reactions used in model calculations (referred to CDOM, nitrate and nitrite), and to the values of scavenging or deactivation rate constants for $^{\bullet}OH$, $CO_3^{-\bullet}$, $^{1}O_2$ and ^{3}CDOM*. All the relevant error sources combine to produce an overall uncertainty that can be assessed at the σ level by use of the file *Apex_Errors.xls* (see ESI).

In that file one should enter the values of direct photolysis quantum yield, second-order reaction rate constants with $^{\bullet}OH$, $CO_3^{-\bullet}$, $^{1}O_2$ and ^{3}CDOM*, and (if available) intermediate formation yields, together with the associated σ-level uncertainty. Afterwards, one can copy and paste into *Apex_Errors.xls* an entire row from an output table, generated by the *savetable* function. Calculations of absolute and relative errors are automatically carried out. It is necessary to copy and paste a whole row and not only single values, because some output variables are needed to calculate errors for the other ones.

3.7 Mid-latitude seasonal trends

The used time unit (SSD) is referred to mid-latitude summertime conditions. The photodegradation kinetics in different seasons is understandably slower,[60] and it can be approximately assessed by using the file *Apex_Season.xls* (see ESI). The main approximation is related to the treatment of direct photolysis, according to which one needs to use different calculation sheets if the target compound mostly absorbs sunlight in the UVB, has an important absorption band in the UVA, or it significantly absorbs visible radiation (the latter is *e.g.* the case of the nitrophenolates reported in Table 1). After choosing the most appropriate sheet, one needs to copy and paste a whole row of an output table (generated by the *savetable* function) to enable approximate calculations of the mid-latitude monthly trends for each output variable. An example of the results that can be obtained by use of the *Apex_Season.xls* file is reported in Figure 4 for atrazine (the ±σ band around the model predictions is obtained by using the *Apex_Errors.xls* file for each monthly value of the half-life time).

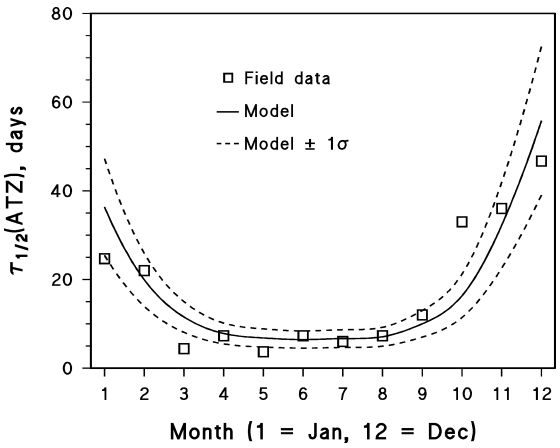

Figure 4. Modelled half-life time of atrazine in different months of the year (unpublished data). Water conditions: 2 mM nitrate, 20 µM nitrite, 1 mg C L^{-1} DOC, 1 mM bicarbonate, 10 µM carbonate, 4.3 m path length of sunlight. Field data are from ref. 61.

One can see that the phototransformation kinetics of atrazine can be around eight times slower in winter than in summer. In this

case the apparent agreement between model predictions and field data [61] should not be overemphasised: incomplete water chemistry information was provided in the reference, and the values of the missing parameters were guessed so as to adapt predictions to field values. An important issue is that, in the case of *Apex_Season.xls*, the time unit is no longer the SSD but rather an average sunny day of the month under consideration.

3.8 Path length of sunlight and water depth: effect of the solar zenith angle

Reflection and refraction phenomena are operational when sunlight crosses the air-water interface. Reflection of sunlight can often be neglected,[21] while refraction deviates the light path towards the vertical (see Figure 5).

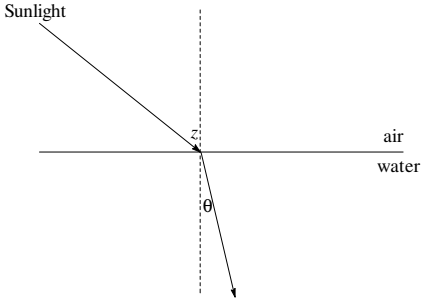

Figure 5. Refraction of sunlight at the air-water interface. The angle of incidence z coincides with the solar zenith angle, while θ is the angle of refraction.

The solar zenith angle z (horizontal system of coordinates) is a function of sun declination δ (geocentric equatorial system of coordinates) and hour angle τ. The latter is the difference between sun's right ascension (geocentric equatorial system of coordinates) and the right ascension of a star on the local meridian. At local noon it is $\tau_{sun} = 0$. Assume φ as the latitude of the place and (δ,τ) for the sun as above. The following equation holds for the solar zenith angle:[62]

$$\cos z = \cos\delta \cos\tau \cos\varphi + \sin\delta \sin\varphi \qquad (16)$$

Water has refraction index $n \sim 1.34$, which undergoes relatively limited variation with wavelength.[21] It is $\sin z = n \sin\theta$, and from the light-path geometry one gets the following relationship between the path length l of sunlight and the water column depth h: $h = l \cos\theta = l \sqrt{1-(\sin\theta)^2}$. By using the solar zenith angle z instead of θ one obtains $h = l\sqrt{1-(n^{-1}\sin z)^2}$. One can thus define $\psi = \left(\sqrt{1-(n^{-1}\sin z)^2}\right)^{-1}$ as the correction factor, by which the water depth h should be multiplied to obtain the sunlight path length l. The latter is the input datum of the *plotgraph* and *savetable* functions. Figure 6 reports the calculated values of ψ at the local noon [63] as a function of the month of the year (15th day of each month), for different values of the latitude.

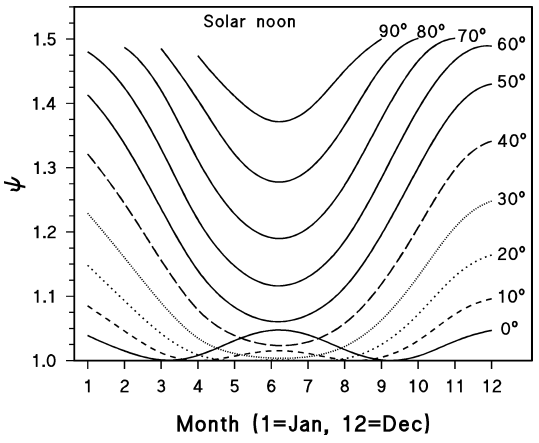

Figure 6. Trend of the correction factor ψ as a function of month and latitude. It is $l = \psi h$ (h = depth, l = path length).

At temperate latitudes during summer, the error made by assuming $\psi \sim 1$ is lower than the uncertainty of the model.

4 Conclusions

The APEX software is derived from a photochemical model that predicts pollutant phototransformation kinetics as a function of photoreactivity parameters (direct photolysis quantum yield and reaction rate constants with $^{\bullet}OH$, $CO_3^{-\bullet}$, $^1O_2$ and $^3CDOM^*$) and of data of water chemistry and depth. The model has been validated by comparison with field data, showing good agreement. APEX is based on the free software *Octave*. By use of model equations, it can produce 3D plots or tables that, as a function of the above parameters, report reactivity data such as half-life times, pseudo-first order rate constants and steady-state concentrations of transients. It is also possible to calculate the kinetics and yields of intermediate formation, based on the relevant yields from the parent compounds *via* the different photochemical pathways. An important issue is that for a defined sunlight path length or water depth, the output values are averages over the whole water column under consideration. Therefore, for *e.g.* 1 m depth, kinetics and steady-state concentrations are referred to the whole 1-m water column (water-column averages) and they are not the point values at the depth of 1 m.

The APEX package, which is provided with this paper as freely available ESI, also includes the files *Apex_Errors.xls* and *Apex_Season.xls*. The former computes the σ-level uncertainty associated with the output data, while the latter gives the (approximate) monthly trend of the output variables. APEX uses as standard time unit a summer sunny day (SSD), equivalent to 15 July at mid-latitude. Therefore, the standard output is referred to summertime irradiation conditions. *Apex_Season.xls* gives insight into the approximate year-round trend of photochemical processes at mid latitude.

This paper gives a general description of APEX, but users should make reference to the more detailed User's Guide that is provided as ESI.

Acknowledgements

DV acknowledges financial support by from Università di Torino

- EU Accelerating Grants, project TO_Call2_2012_0047 (Impact of radiation on the dynamics of dissolved organic matter in aquatic ecosystems - DOMNAMICS).

Notes and references

[a] *MambaSoft, Via Barletta 90, 10136 Torino, Italy.*
[b] *Dipartimento di Chimica, Università di Torino, Via Pietro Giuria 5, 10125 Torino, Italy. http://www.environmentalchemistry.unito.it.*
[c] *Centro Interdipartimentale NatRisk, Università di Torino, Via Leonardo da Vinci 44, 10095 Grugliasco (TO), Italy. http://www.natrisk.org.*

† Electronic Supplementary Information (ESI) available: the file Apex.zip contains the complete APEX package. To run it, the free software *Octave* should first be installed. See DOI: 10.1039/b000000x/

1 P. Boule, D. W. Bahnemann and P. K. J. Robertson (eds.), *Environmental Photochemistry Part II (The Handbook of Environmental Chemistry Vol. 2.M)*, Springer, Berlin, 2005.
2 A. L. Boreen, W. A. Arnold and K. McNeill, *Aquat. Sci.*, 2003, 65, 320-341.
3 W. Wang, O. C. Zafiriou, I. Y. Chan, R. G. Zepp and N. V. Blough, *Environ. Sci. Technol.*, 2007, 41, 1601-1607.
4 S. Canonica and M. Freiburghaus, *Environ. Sci. Technol.*, 2001, 35, 690-695.
5 D. Vione, G. Falletti, V. Maurino, C. Minero, E. Pelizzetti, M. Malandrino, R. Ajassa, R. I. Olariu and C. Arsene, Environ. Sci. Technol., 2006, 40, 3775-3781.
6 S. Halladja, A. Ter Halle, J. P. Aguer, A. Boulkamh and C. Richard, *Environ. Sci. Technol.*, 2007, 41, 6066-6073.
7 B. M. Peterson, A. M. McNally, R. M. Cory, J. D. Thoemke, J. B. Cotner and K. McNeill, *Environ. Sci. Technol.*, 2012, 46, 7222-7229.
8 S. Canonica, T. Kohn, M. Mac, F. J. Real, J. Wirz and U. Von Gunten, *Environ. Sci. Technol.*, 2005, 39, 9182-9188.
9 E. M. White, P. P. Vaughan, R. G. Zepp, *Aquat. Sci.*, 2003, 65, 402-414.
10 P. Borer, B. Sulzberger, S. J. Hug, S. M. Kraemer, R. Kretzschmar, *Environ. Sci. Technol.*, 2009, 43, 1864-1870.
11 D. Vione, J. Feitosa-Felizzola, C. Minero and S. Chiron, *Wat. Res.*, 2009, 43, 1959-1967.
12 A. W. Vermilyea and B. M. Voelker, *Environ. Sci. Technol.*, 2009, 43, 6927-6933.
13 A. Zertal, T. Sehili and P. Boule, *J. Photochem. Photobiol. A: Chem.*, 2001, 146, 37-48.
14 S. Halladja, A. Amine-Khodja, A. ter Halle, A. Boulkamh and C. Richard, *Chemosphere*, 2007, 69, 1647-1654.
15 E. Caupos, P. Mazellier and J. P. Croue, *Wat. Res.*, 2011, 45, 3341-3350.
16 M. Brigante, M. DellaGreca, L. Previtera, M. Rubino and F. Temussi, *Environ. Chem. Lett.*, 2005, 2, 195-198.
17 P. Mazellier, C. Busset, A. Delmont and J. De Laat, *Wat. Res.*, 2007, 41, 4585-4594.
18 G. Ruggeri, G. Ghigo, V. Maurino, C. Minero and D. Vione, *Wat. Res.*, 2013, 47, 6109-6121.
19 M. Minella, M. Rogora, D. Vione, V. Maurino and C. Minero, *Sci. Total Environ.*, 2011, 409, 3463-3471.
20 M. Minella, E. De Laurentiis, O. Buhvestova, M. Haldna, K. Kangur, V. Maurino, C. Minero and D. Vione, *Chemosphere*, 2013, 90, 2589-2596.
21 R. G. Zepp and D. M. Cline, *Environ. Sci. Technol.*, 1977, 11, 359-366.
22 W. J. Cooper, A. C. Jones, R. F. Whitehead and R. G. Zika, *Environ. Sci. Technol.*, 2007, 41, 3728-3733.
23 C. Richard, A. Ter Halle, M. Sarakha, P. Mazellier and J. M. Chovelon, *Actual. Chim.*, 2007, 308, 71-75.
24 S. Canonica, *Chimia*, 2007, 61, 641-644.
25 P. Warneck and C. Wurzinger, *J. Phys. Chem.*, 1988, 92, 6278-6283.
26 M. Fischer and P. Warneck, *J. Phys. Chem.*, 1996, 100, 18749-18756.
27 S. E. Page, W. A. Arnold and K. McNeill, *Environ. Sci. Technol.*, 2011, 45, 2818-2825.
28 B. H. J. Bielski, D. E. Cabelli, R. L. Arudi and A. B. Ross, *J. Phys. Chem. Ref. Data*, 1985, 14, 1041-1100.
29 K. M. G. Mostofa and H. Sakugawa, *Environ. Chem.*, 2009, 6, 524-534.
30 B. Sur, M. Rolle, C. Minero, V. Maurino, D. Vione, M. Brigante and G. Mailhot, *Photochem. Photobiol. Sci.*, 2011, 10, 1817-1824.
31 G. V. Buxton, C. L. Greenstock, W. P. Helman and A. B. Ross, *J. Phys. Chem. Ref. Data*, 1988, 17, 1027-1284.
32 P. L. Brezonik and J. Fulkerson-Brekken, *Environ. Sci. Technol.*, 1998, 32, 3004-3010.
33 F. Wilkinson and J. Brummer, *J. Phys. Chem. Ref Data*, 1981, 10, 809-1000.
34 S. Canonica, U. Jans, K. Stemmler and J. Hoigné, *Environ. Sci. Technol.*, 1995, 29, 1822-1831.
35 S. A. Loiselle, L. Bracchini, A. M. Dattilo and M. Ricci, *Limnol. Oceanogr.* 2009, 54, 590-597.
36 K. Mopper and X. Zhou, *Science*, 1990, 250, 661-664.
37 S. E. Braslavsky, *Pure Appl. Chem.*, 2007, 79, 293-465.
38 V. Maurino, D. Borghesi, D. Vione and C. Minero, *Photochem. Photobiol. Sci.*, 2008, 7, 321–327.
39 U. Kunkel and M. Radke, *Wat. Res.*, 2012, 46, 5551-5565.
40 T. Poiger, H. R. Buser and M. D. Muller, *Environ. Toxicol. Chem.*, 2001, 20, 256-263.
41 L. Bracchini, A. M. Dattilo, V. Hull, S. A. Loiselle, S. Martini, C. Rossi, C. Santinelli and A. Seritti, *J. Photochem. Photobiol. B: Biol.*, 2006, 85, 145-149.
42 A. Albinet, C. Minero and D. Vione, *Chemosphere*, 2010, 80, 759-763.
43 P. R. Maddigapu, M. Minella, D. Vione, V. Maurino and C. Minero, *Environ. Sci. Technol.*, 2011, 45, 209-214.
44 D. Vione, P. R. Maddigapu, E. De Laurentiis, M. Minella, M. Pazzi, V. Maurino, C. Minero, S. Kouras and C. Richard, *Wat. Res.*, 2011, 45, 6725-6736.
45 C. Tixier, H. P. Singer, S. Oellers and S. R. Müller, *Environ. Sci. Technol.*, 2003, 37, 1061-1068.
46 P. R. Maddigapu, D. Vione, B. Ravizzoli, C. Minero, V. Maurino, L. Comoretto and S. Chiron, *Environ. Sci. Pollut. Res.*, 2010, 17, 1063-1069.
47 B. Sur, E. De Laurentiis, M. Minella, V. Maurino, C. Minero and D. Vione, *Sci. Total Environ.*, 2012, 426, 296-303.
48 E. De Laurentiis, S. Chiron, S. Kouras, C. Richard, M. Minella, V. Maurino, C. Minero and D. Vione, *Environ. Sci. Technol.*, 2012, 46, 8164-8173.
49 E. De Laurentiis, M. Minella, M. Bodrato, V. Maurino, C. Minero and D. Vione, *Aquat. Ecosyst. Health Manag.*, 2013, 16, 216-221.
50 L. L. McConnell, J. A. Harman-Fetcho and J. D. Hagy, *J. Environ. Qual.*, 2004, 33, 594-604.
51 G. Marchetti, M. Minella, V. Maurino, C. Minero and D. Vione, *Wat. Res.*, 2013, 47, 6211-6222.
52 S. Canonica, B. Hellrung, P. Muller and J. Wirz, *Environ. Sci. Technol.*, 2006, 40, 6636-6641.
53 J. Wenk and S. Canonica, *Environ. Sci. Technol.*, 2012, 46, 5455-5462.
54 E. De Laurentiis, M. Minella, M. Sarakha, A. Marrese, C. Minero, G. Mailhot, M. Brigante and D. Vione, *Wat. Res.*, 2013, 47, 5943-5953.
55 R. Frank and W. Klöpffer, *Chemosphere*, 1988, 17, 985-994.
56 R. Del Vecchio and N. V. Blough, *Environ. Sci. Technol.*, 2004, 38, 3885-3891.
57 F. Al Housari, D. Vione, S. Chiron and S. Barbati, *Photochem. Photobiol. Sci.*, 2010, 9, 78-86.
58 P. R. Maddigapu, C. Minero, V. Maurino, D. Vione, M. Brigante and G. Mailhot, *Chemosphere*, 2010, 81, 1401–1406.
59 E. De Laurentiis, M. Minella, V. Maurino, C. Minero, G. Mailhot, M. Sarakha, M. Brigante and D. Vione, *Sci. Total Environ.*, 2012, 439, 299-306.
60 S. Huntscha, H. Singer, S. Canonica, R. P. Schwarzenbach and K. Fenner, *Environ. Sci. Technol.*, 2008, 42, 5507-5513.
61 S. W. Chung and R. R. Gu, *Environ. Manag.*, 2009, 44, 46-61.
62 O. Montenbruck and T. Pfleger, *Astronomy on the Personal Computer, 2nd Edition.* Springer, Berlin, 1994.
63 F. Riccio, 2009. http://www.perseus.it.